Robotica (2007) volume 25, pp. 341–349. © 2006 Cambridge University Press
doi:10.1017/S0263574706003134 Printed in the United Kingdom

Designing robot grippers: optimal edge contacts for part alignment

Mike Tao Zhang†,* and Ken Goldberg‡

†*AzFSM (Fab 12/22/32) Industrial Engineering, Intel Corporation, Mail Stop: OC2-254, 4500 S. Dobson Road, Chandler, AZ 85248, USA*
‡*Department of Industrial Engineering and Operations Research and Department of Electrical Engineering and Computer Science, University of California, Berkeley, CA 94720-1777, USA*

(Received in Final Form: October 20, 2006. First published online: November 30, 2006)

SUMMARY
Although parallel-jaw grippers play a vital role in automated manufacturing, gripper surfaces are still designed by trial-and-error. This paper presents an algorithmic approach to designing gripper jaws that mechanically align parts in the vertical (gravitational) plane. We consider optimal edge contacts, based on modular trapezoidal segments that maximize contact between the gripper and the part at its desired final orientation. Given the n-sided 2D projection of an extruded convex polygonal part, mechanical properties such as friction and center of mass, and initial and desired final orientations, we present an $O(n^3 \log n)$ numerical algorithm to design optimal gripper jaws. We also present an $O(n \log n)$ algorithm to compute tolerance classes for these jaws, and report on an online implemented version of the algorithm and physical experiments with the jaws it designed. This paper extends earlier results that generated optimal point contacts [M. T. Zhang and K. Goldberg, "Gripper point contacts for part alignment," *IEEE Trans. Robot. Autom.* **18**(6), 902–910 (2002)].

KEYWORDS: Grasp; Gripper; Geometric Computation; Manipulation.

1. Introduction

"Proper gripper design can simplify the overall assembly, increase the overall system reliability, as well as decrease the implementation cost".[9]

Although grippers are widely used for automated manufacturing, assembly, and packing, there are few geometric algorithms for optimal design of gripper jaw surfaces.

Causey and Quinn[9] suggest several intuitive guidelines for design of jaws: "(1) *grasp parts securely*; (2) *fully encompass the part with the gripper*; (3) *contacts should align grasped parts*; (4) *design for proper gripper–part interaction*; *and* (5) *include functionality in gripper contacts*." Our approach attempts to address these guidelines.

In ref. [40], we showed that it is possible to align parts during grasping using a standard parallel-jaw gripper with four point contacts. We separate the grasp into three phases: pushing, toppling, and fixturing during which it is important to avoid jamming and undesired collision, bringing the part into a form closure configuration where it is held securely. Given an n-sided polygonal part, we presented an $O(n^4)$ numerical algorithm to compute a feasible solution. The algorithm combines toppling, accessibility, and form-closure analysis.

In industrial practice, inertia and disturbances can dislodge point contacts, causing parts to escape from gripper jaws. To improve grasp quality, we extend our earlier approach to maximize contact between the gripper and the part at its desired final orientation.

The inputs of the design problem are the part shape, its COM (Center of Mass), related friction coefficients, and initial and desired orientations of the part. As shown in Fig. 1, the standard industrial parallel-jaw gripper has a pair of two jaws; each jaw consists of a vertical base-plate often with additional machined surfaces. In this paper, we consider a class of trapezoidal jaw modules that are easy to machine. The output of the design problem is an arrangement of trapezoidal jaw modules that rotates the part to the desired orientation and achieves form-closure grasp with maximal edge contacts.

In Section 3, we formally define the problem and in Sections 4–7, we extend the methodology developed in ref. [40] to obtain the optimal edge contacts to improve the quality of the grasp. In Section 8, we address the shape tolerance of the gripper jaws that is defined by a parametric tolerance class. The part alignment is guaranteed for any jaw geometry in the class bounded by maximal and minimal jaw specifications.

To effectively analyze the toppling and motion trajectory, we develop a mathematical framework with innovative geometric functions based on translational/rotational Cartesian frames.

2. Related work

There is a substantial body of research on robotic grasping, see ref. [5] and our previous paper[41] for reviews.

Most relevant to the present paper is recent research on toppling. Lynch[18] derived sufficient mechanical conditions for toppling parts on a conveyor belt in terms of constraints on contact friction, location, and motion. It is possible to orient parts on a conveyor belt by positioning pins (rigid barriers) that topple parts into desired orientations.[38]

*Corresponding author. E-mail: mike.zhang@intel.com

https://doi.org/10.1017/S0263574706003134 Published online by Cambridge University Press

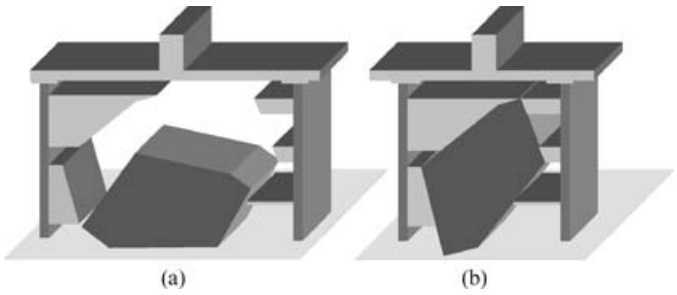


Fig. 1. Gripper with trapezoidal jaw models aligns the part from orientation (a) to orientation (b) as the gripper is closed.

In the following, we review relevant research on tolerancing and online algorithms for mechanical design.

Excellent surveys of tolerancing can be found in refs. [26, 27, 33], and in ref. [35]. Donald[12] studied part manipulation with geometric uncertainty. He considered shape variations as an additional dimension in a generalized configuration space and described multistep error detection and recovery strategies. Abell and Erdmann[1] studied how a planar polygon could be rotated while stably supported by two frictionless contacts. Joskowicz *et al.*[15] presented kinematic tolerance in term of configuration space and developed a worst-case tolerance analysis algorithm for 2-DOF planar pairs. Latombe *et al.*[17] considered an assembly sequence planning problem with toleranced parts. Given a parametric tolerance class, they presented a polynomial time algorithm to decide if an assembly sequence existed. Their tolerance model is similar to ours in that both approaches fix the relative orientation of edges. Akella and Mason[2] developed a planner to generate orienting plans for toleranced polygonal parts. Their tolerance model was defined by circular uncertainty zones around the nominal positions of the COM and the vertices. Chen *et al.*[10] proposed parameteric tolerance classes for sensorless part orienting and fixturing. Each was defined by an uncertainty zone around part vertices. They developed algorithms to compute the boundaries of the tolerance class. Brost and Peters[8] presented an algorithm to design 3D modular fixtures for toleranced parts that were specified by an uncertainty polygon at each vertex. We defined a parametric tolerance class such that self-aligning grasps were guaranteed for all jaw geometry in the class.[37]

Online algorithms for Computer-Aided Design (CAD) are an active research topic. Since the introduction of Java in 1996, a number of geometric algorithms have been made available online. The Geometry Center at the University of Minnesota maintains an extensive collection of interactive geometric algorithms at.(1) The Berkeley Remote Interactive Optimization Testbed (RIOT) includes several online optimization algorithms.(2) Several researchers have developed online CAD software for manufacturing. Wright *et al.*[11,29] developed *Cybercut*(3): a network CAD/CAM service for design and fabrication of mechanical parts on the Internet. Piccinocchi *et al.*[24] presented a Java applet to compare different nonholonomic motion planning algorithms. Goldberg *et al.*,[3,7,34] provided an online fixture design system that finds all modular fixtures for a given part consisting of three locators and one clamp. Cheng *et al.*[16,32] described online CAD tools for CAM and planar mechanical system design at.(4) Berretty *et al.*[4] described an online CAD tool for the design of traps for the tracks of vibratory bowl feeders. Smith *et al.*[30] developed a Java applet to compute and rank all pairs of parallel-jaw grip points for polygonal parts. We described an Internet-based implementation that is available for any Java-enabled Web browser.[41] We also applied this implementation to perform numerical experiments to study conditions under which jaw designs exist. Several papers consider part motion and how it can be used to reduce uncertainty (see refs. [13, 40]).

3. Design problem definition

In this section, we define our problem with input, output, and assumptions and summarize notation.

The inputs of the design problem are the vertices of an n-sided projection of an extruded convex polygonal part, its COM, initial and desired orientations, vertex clearance radius ε, and bounds on the part-surface friction coefficient $[0, \mu_{s_\max}]$ and on the part-gripper friction coefficient $[\mu_{t_\min}, \mu_{t_\max}]$.

The output of the design problem is a report. The report will either state that no solution can be found; or a description of a pair of gripper jaws (specified by a set of trapezoidal jaw modules) that:

Max: (linear) contacts with the part at its desired orientation

Subject to:

1. Orienting the part from the initial orientation to the desired orientation;
2. Achieving a form-closure grasp on the part at its desired orientation.

Without loss of generality, we assume the part rotates counterclockwise. As illustrated in Fig. 2, the pushing tip A' on the left jaw makes contact with the part initially. It pushes the part along the work-surface during the pushing phase until the part makes contact with the toppling tip A on the right jaw. At this moment, the part begins to rotate and the toppling phase starts. The part is constrained by A', A, and the worksurface and is toppled from its initial orientation to the desired final orientation. When the part reaches its final orientation, jaw worksurfaces stop its motion and securely grasp it at the fixturing phase.

Each trapezoidal jaw module is determined by its two vertices that make contact with the part in its final grasp configuration. The line segment between these two vertices is named an *accessible segment*. For each edge of the part, there are 0 or 1 corresponding jaw modules, thus 0 or 1 accessible segments. Our objective is to find the set of accessible segments with maximum total length that allows toppling.

As shown in Fig. 2, the part's COM is a distance ρ from P and an angle η from the $+X$ direction. We define the world frame, $\boldsymbol{W}$, to be a Cartesian coordinate system originating at

(1) http://www.geom.umn.edu/apps
(2) http://riot.ieor.berkeley.edu/
(3) http://cybercut.berkeley.edu/
(4) http://iel.ucdavis.edu/design/

https://doi.org/10.1017/S0263574706003134 Published online by Cambridge University Press

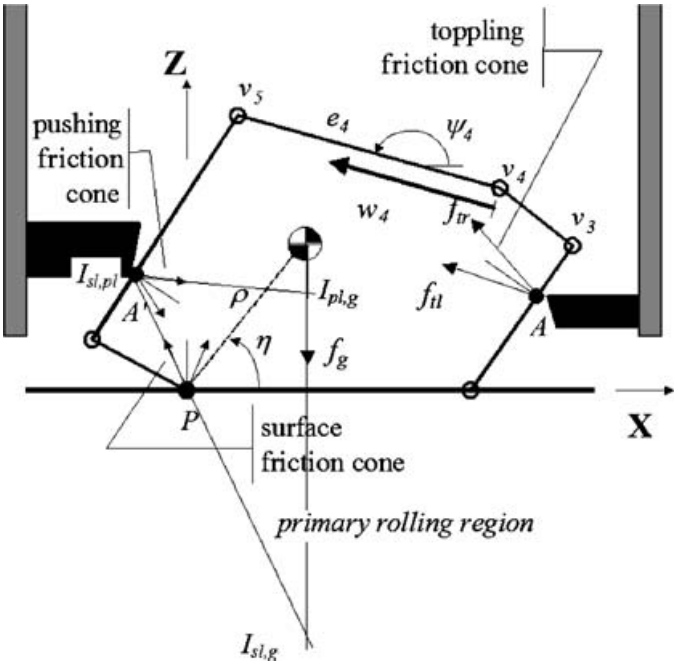


Fig. 2. Side view of polygonal part sitting on a flat worksurface in its stable initial pose.

the pivot point P with X-axis on the worksurface pointing right and Z-axis pointing up. This frame translates to the right as the part is pushed. Let (x_A, z_A) and $(x_{A'}, z_{A'})$ denote the location of A and A', respectively. Starting from P, we consider each edge of the part in counterclockwise order, namely $e_1, e_2, \ldots, e_n$. The edge e_k, with vertices v_k at (x_k, z_k) and $v_{(k+1)}$ at $(x_{(k+1)}, z_{(k+1)})$, is in direction $\psi_k \in [0, 2\pi]$ from the $+X$ axis. Let w_k be the distance along edge e_k. Any point on e_k can be expressed as $(x_k + w_k \cos\psi_k, z_k + w_k \sin\psi_k)$.

During toppling, A and A' make contact with the part and rotate it counterclockwise without being lifted from the worksurface (we derive the sufficient conditions in Section 4). Let F_t, F_p, and F_s denote the contact force at A, A', and P, respectively. We denote the direction at the left edge of the toppling friction cone as f_{tl} (pushing as f_{pl}, worksurface *as* f_{sl}) and the right edge as f_{tr} (pushing as f_{pr}, worksurface *as* f_{sr}). Let f_g denote the vertical line through the part's COM. Let $I_{a,b}$ denote the intersection of line a and line b where a and b can be anyone of $f_{tl}, f_{pl}, f_{sl}, f_{tr}, f_{pr}, f_{sr}, f_g f_t, f_p$, and f_s. We denote P_0 as $I_{sl,pl}$, P_1 as $I_{sl,g}$, and P_2 as $I_{pl,g}$. Let θ denote the rotational angle of the part as measured from the x-axis. Initially $\theta = 0$; θ_D is the part's desired orientation. We say an edge e_k is *visible* if it can be seen from $+X$ direction; otherwise, it is *invisible*. Thus, e_k is visible if $0 < \psi_k + \theta < \pi$; e_k is invisible if $\pi < \psi_k + \theta < 2\pi$.

The part motion on the worksurface during the grasp consists of two aspects: rotation and linear translation. To facilitate detailed study, we decompose it into pure rotation and pure linear translation. The part first rotates about P to *semiposition*, and then translates to *actual-position*. Let $(x_{j,\theta}, z_{j,\theta})$ and $(x'_{j,\theta} \cdot z'_{j,\theta})$ denote the actual-position and the semiposition, respectively, of vertex v_j at θ. Let $(x_{j,D}, z_{j,D})$ and (x'_j, D, z'_j, D) denote the actual-position and the semiposition, respectively, of vertex v_j at θ_D.

A motion of the part can be represented by the center-of-rotation and the direction of rotation. In the x–z plane, the direction of a contact force divides the plane into two halves. We sign the half-plane positive if it obeys the right-hand rule pointing inward and the other half-plane negative. If the overlapped zone of the positive half-planes for F_s, F_p, and M_g is a closed geometric shape, we name it the *primary rolling region*. Rolling is guaranteed if F_t makes a counterclockwise moment about the primary rolling region.[20,31]

We assume the following throughout the paper: both parts and grippers are rigid; part geometry and location of the COM are known; part motion is sufficiently slow enough to ignore inertial effects; the part extrusion axis is perpendicular to the motion of the jaws; and parts reach final desired orientation before any edge lies on the worksurface. Without loss of generality, we assume that the part will be rotated counterclockwise. Jaw tips for clockwise rotation can be computed using a mirror image of the part. Due to lack of space, we also use single-valued part-surface and part-jaw friction coefficients, μ_s and μ_t (their corresponding friction cone half-angle being α_s and α_t, respectively). The solutions for the bounded friction coefficient range can be obtained by the method described in ref. [40]

4. Grasping mechanics

In this section, we describe how to determine the heights of A' and A such that the part on the worksurface will be rotated to the desired orientation.

During pushing, A' touches the part first and pushes the part on the worksurface till both A' and A make contact with the part. To guarantee the linear translation of the part on the worksurface, neither rolling nor jamming may occur. We derive the conditions to prevent jamming and rolling in this phase.[36] During toppling, it is important to guarantee that the part remains in contact with A, A', and the worksurface.

Let θ_T denote the critical part orientation beyond which the part will lose contact with the worksurface and rotate around A'. To solve for θ_T, we find the critical angle where the part's COM is straight above A'. Thus, we have $x_{A'} = \rho \cos(\eta + \theta_T)$, i.e., $\theta_T = \cos^{-1}(x_{A'}/\rho) - \eta$.

The part rotates about P and slides to the right continuously. Thus, F_s is in the direction of f_{sl}. By examining the kinematics of the part and the jaw during rotation, we can determine which direction the tips slide relative to the part. This knowledge allows us to limit our consideration to one edge of the friction cones. In general, the direction of these forces depends on the X coordinate of the contact. We proved that F_t is in the direction of f_{tl} if $x_A > 0$, f_{tr} if $x_A < 0$; F_p is in the direction of f_{pr} if $x_{A'} > 0$; f_{pl} if $x_{A'} < 0$.[39]

During toppling, the part rotates and translates relative to three contacts: A', A, and P. The system of forces on the part, M_g, F_p, F_t, and F_s, must generate a counterclockwise moment with respect to P. Given that $z_{A'}$ and A are in contact with edge e_j, the rolling function $H_j(\theta)$ is the minimum height of A that guarantees to roll the part instantaneously at θ.

If $x_{A'} > 0$, F_p is in the direction of f_{pr}; if $x_{A'} < 0$, F_p is in the direction of f_{pl}. We apply the same method to find the rolling function.[39] We focus on $x_{A'} < 0$ in this paper. Draw a line at A' parallel to f_{sl} and intersecting f_g at a critical point $\boldsymbol{C}$. As shown in Fig. 3, the existence of the primary rolling region is determined by the relative position of $I_{pl,g}$ and $\boldsymbol{C}$.

https://doi.org/10.1017/S0263574706003134 Published online by Cambridge University Press

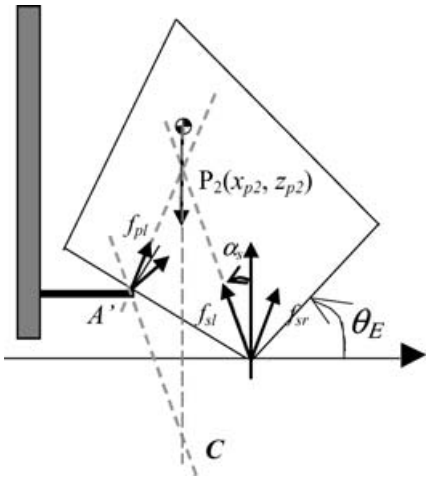


Fig. 3. θ_E: Critical angle where sliding starts.

If $I_{pl,g}$ is above C: $\psi_i > \pi + \alpha_s - \alpha_t$. There exists a primary rolling region: triangle $P_0P_1P_2$. $P_0(x_{p0}, z_{p0})$ is $I_{sl,pl}$, P_1 (x_{p1}, z_{p1}) is $I_{sl,g}$, and $P_2(x_{p2}, z_{p2})$ is $I_{pl,g}$. We have:

$$x_{p0} = \frac{\mu_s x_{A'} \tan\gamma_{il} - \mu_s z_A}{1 + \mu_s \tan\gamma_{il}},\ z_{p0} = \frac{-x_{A'} \tan\gamma_{il} + z_{A'}}{1 + \mu_s \tan\gamma_{il}},$$

$$x_{p1} = t, z_{p1} = -\frac{t}{\mu_s}, x_{p2} = t, z_{p2} = (t - x_{A'}) \tan\gamma_{il} + z_{A'},$$

where $\gamma_{il} = \psi_i + \alpha_t + \theta + \pi/2$ and $t = \rho\cos(\eta + \theta)$.

If f_{tl} passes above the triangle, f_{tr} will pass higher and generate a clockwise moment about the triangle. Moreover, we assume that the angle between f_{tr} and f_{tl}, which is $2\alpha_t$, is small considering metal parts and jaws. Thus, we consider a conservative solution and find the height sufficient to roll the edge by projecting lines from P_0, P_1, and P_2 along angle f_{tl} into the edge contacting A. The intersection with the maximum height of those three is the minimum height needed to roll the part.

Let $w_{j,0}$ denote the toppling contact on a visible edge e_j where f_{tl} passes exactly through point P_0. We can show through geometric construction that:

$$w_{j,0}(\theta) = \frac{z'_{j,\theta} - z_{p0} - (x'_{j,\theta} - x_{p0}) \tan\gamma_{jl}}{\cos\xi_j \tan\gamma_{jl} - \sin\xi_j},$$

where $\xi_j = \theta + \psi_j$ and $\gamma_{jl} = \psi_j + \alpha_t + \theta + \pi/2$.

Similarly, the edge contacts for f_{tl} passing through P_1 and P_2 are given by $w_{j,1}(\theta)$ and $w_{j,2}(\theta)$:

$$w_{j,1}(\theta) = \frac{z'_{j,\theta} - z_{p1} - (x'_{j,\theta} - x_{p1}) \tan\gamma_{jl}}{\cos\xi_j \tan\gamma_{jl} - \sin\xi_j}, \text{ and}$$

$$w_{j,2}(\theta) = \frac{z'_{j,\theta} - z_{p2} - (x'_{j,\theta} - x_{p2}) \tan\gamma_{jl}}{\cos\xi_j \tan\gamma_{jl} - \sin\xi_j}.$$

Thus, the rolling function is given by

$$H_j(\theta) = \begin{cases} H_j^*(\theta) & H_j^*(\theta) \geq V_j(\theta) \\ 0 & H_j^*(\theta) < V_j(\theta) \end{cases},$$

where $H_j^*(q) = x_j \sin\theta + z_j \cos\theta + w_j(\theta) \sin(\psi_j + \theta)$ and $w_j(\theta)$ is the maximum of $w_{j,0}$, $w_{j,1}$, and $w_{j,2}$, which can be shown to be

$$w_j(\theta) = \begin{cases} w_{j,2}(\theta) & 0 < \theta < \theta_{01} \text{ and } \psi_j < \phi \\ w_{j,0}(\theta) & 0 < \theta < \theta_{01} \text{ and } \psi_j \geq \phi \\ \infty & \text{otherwise,} \end{cases}$$

where $\phi = \psi_i + \pi$, $\theta_{01} = \pi + \alpha_s - \alpha_t - \psi_j$.

If $I_{pl,g}$ is below C: no primary region exists; thus let $H_j(\theta) = \infty$.

As the part rotates, it may accelerate under gravity and lose contact with A. We now define another critical angle, θ_E, where the part remains stationary with only contacts at A' and P. This angle corresponds to the angle where P_2 is on the left edge of the surface friction cone; i.e., the vertical line through the COM, the left edge of the surface friction cone, and the left edge of the pushing friction cone intersect at the same point. As shown in Fig. 3, we use the following equation to solve for θ_E:

$$\tan(\alpha_s) = \left|\frac{x_{p2}}{z_{p2}}\right| = \left|\frac{\rho\cos(\eta + \theta_E)\tan(\psi_i + \alpha_t + \theta_E)}{z_{A'}\tan(\psi_i + \alpha_t + \theta_E) - \rho\cos(\eta + \theta_E) + x_{A'}}\right|.$$

If the desired final rotational angle is larger than θ_E, we cannot guarantee the outcome and therefore must report that no solution exists. Therefore, $\theta_D \in [0, \min(\theta_T, \theta_E)]$ must be satisfied to guarantee that the part remains in contact with A, A', and the worksurface.

We develop *toppling function*: a vector of geometric functions that maps from part orientation to the height of A: $\boldsymbol{S}^1 \rightarrow \Re^+$, where $\boldsymbol{S}^1$ is the set of planar orientations based on the rotational angle θ. It combines the vertex functions and the rolling functions for the visible edges over the range $\theta \in [0, \min(\theta_T, \theta_E)]$. From the toppling function, the height of A (which is capable of rotating the part to the desired orientation) can be determined or shown to be nonexistent.[40]

5. Motion trajectory analysis

Once the part reaches the desired orientation θ_D, the jaws must terminate its rotation and grasp it with maximal contact. There exists an accessibility constraint due to the fact that the jaws should not block the part motion during toppling. In this section, we will derive the condition to guarantee that the gripper jaws would not obstruct the motion trajectory of the part.

We first consider the motion trajectory of the visible edges. Considering the relative motion, we take the toppling contact as a fixed point; therefore, the part motion is constrained by A and the worksurface as shown in Fig. 4. The motion trajectories of the invisible edges can be obtained by the same method (taking A' as a fixed point).

Our analysis involves *quasi-vertex functions* that represent the motion trajectory of vertices as the part rotates. The quasi-vertex function helps us to study how the part vertices and edges move during the grasp so that we can design the jaws

https://doi.org/10.1017/S0263574706003134 Published online by Cambridge University Press

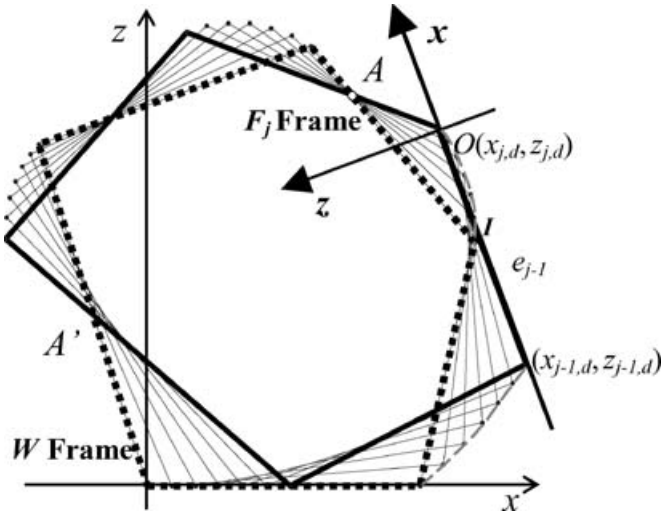


Fig. 4. Part motion trajectory: *Dotted/solid lines* indicate the initial/final orientation of the part and *dashed lines* represent the motion trajectories of vertices.

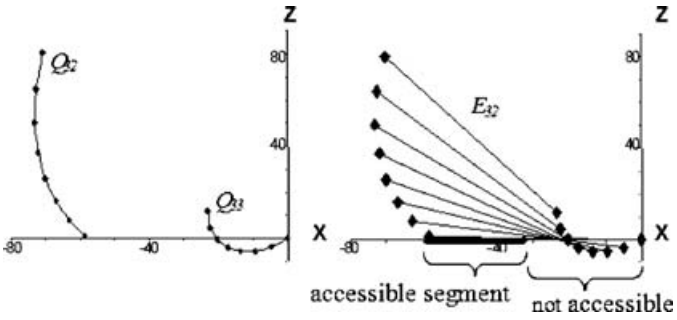


Fig. 5. Quasi-vertex functions for the part in Fig. 4 given $z_A = 3.65$.

to not block the motion of the part. To obtain the function, we define a frame of reference $\boldsymbol{F_j}$ at the desired orientation of the part. As shown in Fig. 4, $\boldsymbol{F_j}$ originates at v_j; the x-axis of $\boldsymbol{F_j}$ overlaps with edge $e_{(j-1)}$ pointing to v_j; and the z-axis of $\boldsymbol{F_j}$ is the interior normal of edge $e_{(j-1)}$. Therefore, the frame $\boldsymbol{F_j}$ rotates with the part during toppling. The quasi-vertex function $Q_{jk}(\theta, z_A)$ indicates the location of v_k in $\boldsymbol{F_j}$ at θ.

We apply a homogeneous transformation to obtain the quasi-vertex function. First, we derive ${}^{Fj}\boldsymbol{T_W}$, which is a transformation matrix from the frame $\boldsymbol{W}$ to $\boldsymbol{F_j}$. Then, we find the motion trajectory of v_k in $\boldsymbol{W}$. Finally, we map the motion trajectory of v_k from $\boldsymbol{W}$ to $\boldsymbol{F_j}$. Let $x_{t,\theta}$ and $x_{t,D}$ denote the horizontal distance between the actual-position and the semiposition of any point on the part at θ and θ_D, respectively, i.e., $x_{t,\theta} = x_{A,\theta} - x'_{A,\theta}$ and $x_{t,D} = x_{A,D} - x'_{A,D}$.

We describe the motion trajectory of vertex v_k in $\boldsymbol{W}$ numerically. At each θ, we compute the position of v_k

$$\boldsymbol{V_W} = \boldsymbol{Rot}(y, -q)\boldsymbol{Trans}(x_{t,\theta}, 0, 0)\begin{bmatrix} x_k \\ 0 \\ z_k \\ 1 \end{bmatrix}$$

$$= \begin{bmatrix} x_k \cos\theta - z_k \sin\theta + x_{t,\theta} \\ 0 \\ x_k \sin\theta + z_k \cos\theta \\ 1 \end{bmatrix},$$

where $x_{t,\theta} = x_A - \frac{(z_A - z'_{l,\theta})(x'_{l+1,\theta} - x'_{l,\theta})}{z'_{l+1,\theta} - z'_{l,\theta}} - x'_{l,\theta}$ if $z'_{l,\theta} < z_A < z'_{l+1,\theta}$. We map the motion trajectory of v_k in $\boldsymbol{W}$ into $\boldsymbol{F_j}$ to obtain

$$Q_{jk}(\theta) = {}^{Fj}\boldsymbol{T_W}\boldsymbol{V_W} = \begin{bmatrix} Q_{jk,x}(\theta, z_A) \\ Q_{jk,z}(\theta, z_A) \end{bmatrix} = \begin{bmatrix} (x'_{k,\theta} - x'_{j,D} + x_{t,\theta} - x_{t,D})\cos(\psi_{j-1} + \theta_D) + (z'_{k,\theta} - z'_{j,D})\sin(\psi_{j-1} + \theta_D) \\ -(x'_{k,\theta} - x'_{j,D} + x_{t,\theta} - x_{t,D})\sin(\psi_{j-1} + \theta_D) + (z'_{k,\theta} - z'_{j,D})\cos(\psi_{j-1} + \theta_D) \end{bmatrix}.$$

$${}^{W}\boldsymbol{T}_{Fj} = \boldsymbol{Trans}(x'_{j,D}, 0, z'_{j,D})\boldsymbol{Trans}(x_{t,D}, 0, 0)\boldsymbol{Rot}(y, -(\psi_{j-1} + \theta_D))$$

$$= \begin{bmatrix} \cos(\psi_{j-1} + \theta_D) & 0 & -\sin(\psi_{j-1} + \theta_D) & x'_{j,D} + x_{t,D} \\ 0 & 1 & 0 & 0 \\ \sin(\psi_{j-1} + \theta_D) & 0 & \cos(\psi_{j-1} + \theta_D) & z'_{j,D} \\ 0 & 0 & 0 & 1 \end{bmatrix},$$

where $x_{t,D} = x_A - \frac{(z_A - z'_{m,D})(x'_{m+1,D} - x'_{m,D})}{z'_{m+1,D} - z'_{m,D}} - x'_{m,D}$ if $z'_{m,D} < z_A < z'_{m+1,D}$. So the transformation matrix ${}^{Fj}\boldsymbol{T_W}$ is given by

$${}^{Fj}\boldsymbol{T_W} = \left[{}^{W}\boldsymbol{T}_{Fj}\right]^{-1} = \begin{bmatrix} \cos(\psi_{j-1} + \theta_D) & 0 & \sin(\psi_{j-1} + \theta_D) & -(x'_{j,D} + x_{t,D})\cos(\psi_{j-1} + \theta_D) - z'_{j,D}\sin(\psi_{j-1} + \theta_D) \\ 0 & 1 & 0 & 0 \\ -\sin(\psi_{j-1} + \theta_D) & 0 & \cos(\psi_{j-1} + \theta_D) & +(x'_{j,D} + x_{t,D})\sin(\psi_{j-1} + \theta_D) - z'_{j,D}\cos(\psi_{j-1} + \theta_D) \\ 0 & 0 & 0 & 1 \end{bmatrix}.$$

As illustrated in Fig. 5 (where $j = 3$ and $k = 2$), the line segment between $Q_{jk}(\theta, z_A)$ and $Q_{j(k+1)}(\theta, z_A)$ in the same rotational angle θ represents the corresponding configuration of edge e_k in $\boldsymbol{F_j}$. We refer it as to $E_{jk}(\theta, z_A)$. It intersects the x-axis of $\boldsymbol{F_j}$ at $X_j = \frac{(Q_{jk,x} - Q_{j(k+1),x})Q_{jk,z}}{Q_{j(k+1),z} - Q_{jk,z}} + Q_{jk,x}$, if $Q_{jk,z} \cdot Q_{j(k+1),z} < 0$. The portion of edge $e_{(j-1)}$ is accessible if it does not intersect $E_{jk}(\theta, z_A)$ at different θ's. We obtain the accessible segment on edge $e_{(j-1)}$ by eliminating all the intersections between $E_{jk}(\theta, z_A)$ and the x-axis of $\boldsymbol{F_j}$.

6. Form-closure analysis

We also require that the set of the accessible segments must generate a form-closure grasp on the part.

We rename the endpoints of the accessible segments (x_1, z_1), $(x_2, z_2), \ldots, (x_m, z_m)$. Let V_k denote the unit-normal inward vector at (x_k, z_k), V_{kx} (V_{kz}) denote the $x(z)$-axis

https://doi.org/10.1017/S0263574706003134 Published online by Cambridge University Press

projection of the vector at (x_k, z_k), and T_k denote the torque of V_k. Thus, the *Wrench matrix*

$$\mathbf{Wr} = \begin{bmatrix} V_{1x} & V_{2x} & V_{3x} & \dots & V_{mx} \\ V_{1z} & V_{2z} & V_{3z} & \dots & V_{mz} \\ T_1 & T_2 & T_3 & \dots & T_m \end{bmatrix}.$$

The *wrench space* is a 3-dimensional manifold defined by V_x, V_z, and T. Each column of **Wr** represents a point in the wrench space. Mishra *et al.*[21] proved that a form-closure grasp is guaranteed if the origin of the wrench space lies strictly in the convex hull of these points.

We develop the following algorithm to check the form-closure: Compute wrench matrix **Wr**; Define the set of points, **Q**, in wrench space by each column of **Wr** and the origin of wrench space ***O***; Find the convex hull of **Q**, ***CH***(**Q**); If ***O*** is inside ***CH***(**Q**), the set of the accessible segments achieve form-closure on the part.

Since it takes a time of $O(m \log m)$ to construct the 3D convex hull of m points[25] and $m \leq 2n$, the running time to check the form-closure of the set of accessible segments is $O(n \log n)$.

7. Algorithm

To ensure the stability of a grasp, A' and A have to stay at least ε (Safety Zone) units away from the part vertices. We develop the following numerical algorithm:

1. **Find the highest vertex v_p in part's initial orientation**
2. **Define set of invisible edges, $\mathbf{I} = \{$edge $e_i \mid p \leq i \leq n\}$; set of visible edges, $\mathbf{V} = \{$edge $e_j \mid 1 < j < p\}$**
3. **For each invisible edge $e_i \in \mathbf{I}$**
   Compute set of k uniformly spaced sample points, $\mathbf{K_I}$
   For each sample point $A' \in \mathbf{K_I}$
   Check if A' is out of safety zone ε
   Check if A' satisfies pushing condition
   Compute Toppling Function given A'
   For each visible edge $e_j \in \mathbf{V}$
   Compute set of k uniformly spaced sample points, $\mathbf{K_V}$
   For each sample point $A \in \mathbf{K_V}$
   Check if A is out of safety zone ε
   Check if A satisfies nonliftoff condition
   Check if (A, A′) satisfies toppling condition
   Perform accessibility analysis to obtain R(A, A′): a set of accessible segments
   Check if R(A, A′) achieves form-closure
   Output S: set of all R(A, A′) with form-closure
4. **Output $R(A, A')$ with the maximal total length in S**

We found that $k = 10$ works well in practice for the parts we tested. An asymptotic upper bound of the algorithm's running time can be derived as follows.

We find the highest vertex v_p in the part's initial orientation by comparing the heights of all vertices. Thus, Step 1 takes time $O(n)$.

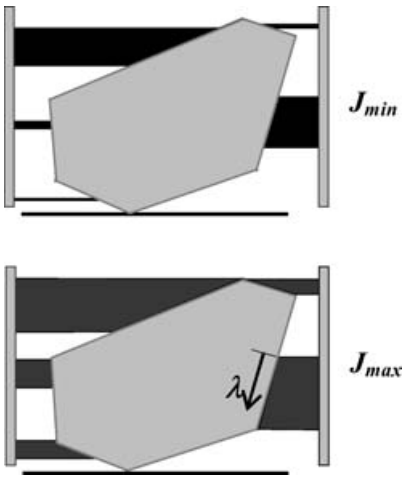


Fig. 6. Parametric tolerance class for robot gripper jaws is defined by jaws with minimal and maximal contact area.

Given an n-sided polygonal part, there are $O(n)$ invisible edges and $O(n)$ visible edges at the initial orientation of the part, i.e., $|\mathbf{I}| = O(n)$ and $|\mathbf{V}| = O(n)$.

We sample each invisible edge into k uniform-distributed points. For each of these points (i.e., the pushing contact A'), we check if it is out of the vertex safety zones and if it satisfies the pushing condition in time $O(n)$. We then compute the toppling function for given A' in time $O(n)$. Next, we sample each visible edge into k uniform-distributed points. For each of these points (i.e., the toppling contact A), we check to see if it is out of the vertex safety zones in time $O(n)$. For the pair of (A, A'), we apply the toppling function to test if the toppling condition is satisfied in time $O(n)$. Then, we find a set of accessible segments, called $R(A, A')$, in time $O(n)$ and check form-closure in time $O(n \log n)$. This step outputs $\boldsymbol{S}$, which is the set of all $R(A, A')$'s that can topple the part and grasp it in form-closure. Hence, Step 3 takes time $O(n)$ $k\ \{O(n) + O(n)\ k\ [O(n) + O(n) + O(n \log n)]\} = O(k^2\ n^3 \log n)$.

In Step 4, we find the optimal solution, which is $R(A, A')$ with the maximal total length in $\boldsymbol{S}$. Since there are $O(k^2\ n^2)$ pairs of (A, A'), this step takes time $O(k^2\ n^2)$.

Therefore, the total running time for the algorithm is $O(n) + O(k^2\ n^3 \log n) + O(k^2\ n^2) = O(k^2\ n^3 \log n)$.

8. Geometric tolerance

For many industrial applications, it may be preferable to use jaws with smaller contact area, for example, to minimize gripper weight for high-velocity transfer. Furthermore, machined jaws may not precisely comply with the specified maximal contact geometry. In this section, we consider variations in jaw shape and define a tolerance class based on maximal and minimal contact areas.

We assume perfect form: all trapezoidal jaw modules in the tolerance class have perfect linear edges. We define the tolerance class by fixing A and A' and computing how far the other jaw module boundaries can move. As illustrated in Fig. 6, we define a single common tolerance parameter λ along the part-jaw contact of all the jaw modules.

https://doi.org/10.1017/S0263574706003134 Published online by Cambridge University Press

We consider jaw module geometry $\boldsymbol{J}$ defined by λ, and let $\boldsymbol{J}_{\max}$ ($/\boldsymbol{J}_{\min}$) denote the maximal (/minimal) contact geometry that is able to topple the part and achieve a form-closure grasp. $[\boldsymbol{J}_{\min}, \boldsymbol{J}_{\max}]$ defines a tolerance class: the uncountable set of grippers with jaws having edges parallel to $\boldsymbol{J}_{\min}$ and $\boldsymbol{J}_{\max}$ and volume within these lower and upper boundaries. Figure 6 illustrates $\boldsymbol{J}_{\min}$ and $\boldsymbol{J}_{\max}$ for a given part: both align the part to the desired orientation and achieve a form-closure grasp on the part. Therefore, a tolerance class contains all the feasible designs of the jaw.

8.1. Tolerance problem definition

Let $\mathbf{I}$ denote the input to the optimal jaw design algorithm defined in the previous sections. We consider two problems:

(1) Given $<\mathbf{I}, \boldsymbol{J}>$, is $\boldsymbol{J}$ *feasible* (will it rotate the part and grasp it in form-closure)? The output of the problem is binary: yes if $\boldsymbol{J}$ is feasible; no if not.
(2) Given $<\mathbf{I}, \boldsymbol{J}_{\max}>$, how to determine the tolerance class? The output of the problem is $\boldsymbol{J}_{\min}$.

8.2. Feasible jaw geometry

To solve Problem (1)—checking if a given $\boldsymbol{J}$ is feasible, we develop an $O(n \log n)$ algorithm as follows:

1. Test if $\boldsymbol{J}$ achieves form-closure in time $O(n \log n)$.
2. Test if $\boldsymbol{J}$ is able to rotate the part to the desired final orientation in time $O(n)$.
   2.1 Find A and A', which are the only vertices that keep touch with the part during toppling;
   2.2 Known A', we construct the corresponding toppling function and check if the pair of (A, A') can rotate the part to the final orientation.
3. Check if any portion of $\boldsymbol{J}$ will block the part's motion trajectory. If the accessible segment of each jaw module of $\boldsymbol{J}$ is shorter than that of $\boldsymbol{J}_{\max}$, no portion of the jaws will become an obstacle to the trajectory.

8.3. Tolerance class

We first prove the convexity of the tolerance class: if $\boldsymbol{J} \in [\boldsymbol{J}_{\min}, \boldsymbol{J}_{\max}]$, $\boldsymbol{J}$ must be feasible. Then, we describe an algorithm to find $\boldsymbol{J}_{\min}$ by searching the upper bound of λ.

Lemma 1. If $\boldsymbol{J} \in [\boldsymbol{J}_{\min}, \boldsymbol{J}_{\max}]$, $\boldsymbol{J}$ must be feasible.

Proof: Both $\boldsymbol{J}_{\min}$ and $\boldsymbol{J}_{\max}$ are feasible by definition. If $\boldsymbol{J}$ is feasible, it must be able to topple the part to the desired orientation and achieve a form-closure grasp on the part at its desired orientation. Let's study these two problems, respectively.

(1) Can $\boldsymbol{J}$ topple the part to the desired orientation?

First, we consider the toppling conditions. Since A and A' are fixed for all $\boldsymbol{J}$ in the class, the toppling condition of $\boldsymbol{J}$ is the same as that of $\boldsymbol{J}_{\max}$. Since $\boldsymbol{J}_{\max}$ satisfies the toppling conditions, $\boldsymbol{J}$ must also satisfy them. Second, we consider the part's motion trajectory conditions. Since $\boldsymbol{J}$ is smaller than $\boldsymbol{J}_{\max}$, it cannot block the motion trajectory of the part. Thus, $\boldsymbol{J}$ is able to topple the part to the desired orientation.

(2) Can $\boldsymbol{J}$ achieve a form-closure grasp on the part at its desired orientation?

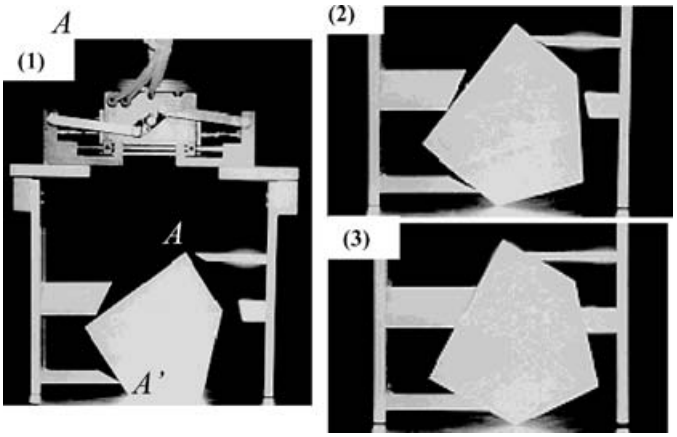


Fig. 7. A successful experiment for $J_{\min}$: (1) Before the grasp; (2) toppling phase; and (3) fixturing phase.

$\boldsymbol{J}$ is larger than $\boldsymbol{J}_{\min}$. Since $\boldsymbol{J}_{\min}$ achieves a form-closure grasp on the part, $\boldsymbol{J}$ must have the same property.

In summary, $\boldsymbol{J}$ can topple the part to the desired orientation and achieve a form-closure grasp on it. Thus, $\boldsymbol{J}$ is feasible.

8.3.1. Numerical algorithm. We use a binary search to find the maximal λ. We choose a small positive number δ. Starting with $\lambda = \delta$, we use the algorithm for Problem (1) to check if the corresponding $\boldsymbol{J}$ is feasible. If so, we try $\lambda = 2\delta$, and so on, until λ is sufficiently large enough that $\boldsymbol{J}$ is no longer feasible. We then interpolate to a desired level of accuracy to find $\boldsymbol{J}_{\min}$.

9. Implementation

We implement the jaw design algorithm into a Java-based CAD tool over the Internet to provide rapid feedback to designers. The user interface of the implementation is shown in ref. [41]. Users can draw a convex polygonal part (up to 10 sides) with a mouse, drag it from the initial resting pose to the desired orientation, and view the optimal jaw design (if any exist). The algorithm requires approximately 7–10 s to find and rank jaw designs on a 266 MHz Pentium II PC.

We also conducted physical experiments to verify our algorithms using an *AdeptOne* industrial robot and a pneumatic parallel-jaw gripper. A part and two sets of jaws were machined from aluminum stock. The friction coefficients are $m_t = [0, 0.1]$ and $\mu_s = [0, 0.1]$.

The sample part is initially in the stable orientation, and we desire to rotate the part 20° to the desired final orientation. We run the jaw design algorithm and find $\boldsymbol{J}_{\max}$ as shown in ref. [41]. We also apply the tolerance algorithm to find the upper bound of λ and $\boldsymbol{J}_{\min}$ as shown in Fig. 7, where only A' and A make contacts with the part before the fixturing phase. We installed these two sets of the jaws onto the robot. We tested each $\boldsymbol{J}_{\max}$ and $\boldsymbol{J}_{\min}$ over 50 trials to grasp the part and observed zero failures. Figure 7 illustrates, in sequence, $\boldsymbol{J}_{\min}$ successfully rotating the part to the desired orientation and grasping it securely.

https://doi.org/10.1017/S0263574706003134 Published online by Cambridge University Press

10. Discussion and conclusion

In industrial practice, gripper jaw geometry is often custom-designed and machined for each part. Design has been ad-hoc and particularly challenging when the part's natural resting pose differs from the desired grip/insertion pose.

In this paper, we present an algorithm to design optimal gripper jaws to align the part and grasp it in form-closure. We identify translational/rotational Cartesian frames and new geometric functions to graphically study the mechanism of toppling, motion trajectory, and form closure. We present a polynomial-time algorithm to find the gripper jaw design and also the parametric tolerance class. We performed physical experiments to confirm the performance of one design generated by the algorithm and have made the algorithm publicly accessible via a Java applet at: http://goldberg.berkeley.edu/sa-gripper/.

In future research, we hope to extend this algorithm to consider design of jaws that can grasp two or more parts, polygonal parts with concavities, to 3D polyhedral parts, and deformable and toleranced parts.

Acknowledgments

Preliminary research on these ideas was reported in refs. [36, 37, 39, 40]. We would like to thank the anonymous reviewers for their careful review of this paper. We also would like to thank Prof. Ilan Adler (IEOR) and Prof. John Canny (EECS) at UC Berkeley for their feedback on Mike Tao Zhang's PhD dissertation. This work was supported in part by the National Science Foundation under DMI-0010069, CDA-9726389, and Presidential Faculty Fellow Award IRI-9553197. Research funding was also provided by Adept Technology, Inc., Ford Motor Co., and California State MICRO Grant 00-032. Thanks also go to Sean Sweat at MIT and Kimberly Bryant at Intel Corporation for helpful comments.

References

1. T. Abell and M. Erdmann, "Stably supported rotations of a planar polygon with two frictionless contacts," *Proceedings of the IEEE/RSJ International Conference on Intelligent Robots Systems*, Pittsburgh, PA (1995) pp. 411–418.
2. S. Akella and M. Mason. "Orienting toleranced polygonal parts," *Int. J. Robot. Res.* **19**(12), 1147–1170 (2000).
3. C. Anderson, Y. Zhuang and K. Goldberg. "Fixturenet II: Interactive redesign and force visualization on the Web (CD)," *Proceedings of the ASME Design Engineering Technical Conference*, Sacramento, CA (1997).
4. R.-P. Berretty, K. Goldberg, L. Cheung, M. Overmars, G. Smith and A. F. Van Der Stappen. "Trap design for vibratory bowl feeders," *Proceedings of the IEEE International Conference on Robotics and Automation*, Detroit, MI (1999), pp. 2558–2563.
5. A. Bicchi, "Hands for dexterous manipulation and robust grasping: A difficult road toward simplicity," *IEEE Trans. Robot. Autom.* **16**(6), 652–662 (2000).
6. S. Brown and P. Wright, "A progress report on the manufacturing analysis service, an Internet-based reference tool," *J. Manuf. Syst.* **17**, 389–398 (1998).
7. R. Brost and K. Goldberg, "A complete algorithm for designing planar fixtures using modular components," *IEEE Trans. Robot. Autom.* **12**(1), 31–46 (1999).
8. R. Brost and R. Peters, "Automatic design of 3-D fixtures and assembly pallets," *Int. J. Robot. Res.* **17**(12), 1243–1281 (1998).
9. G. Causey and R. Quinn, "Gripper design guidelines for modular manufacturing," *Proceedings of the IEEE International Conference on Robotics and Automation*, Leuven, Belgium (1998), pp. 1453–1458.
10. J. Chen, K. Goldberg, M. Overmas, D. Halperin, K. Bohringer and Y. Zhuang, "Shape tolerance in feeding and fixturing," In: *Robotics: The Algorithmic Perspective* (P. Agarwal, L. Kavraki and M. Mason, eds.) (A. K. Peters, Natick, MA, (1999).
11. W. Chui and P. Wright, "A WWW computer integrated manufacturing environment for rapid prototyping and education," *J. Comput. Integr. Manuf.* **12**, 54–60 (1999).
12. B. Donald, "Planning multistep error detection and recovery strategies," *Int. J. Robot. Res.* **9**(1), 3–60 (1990).
13. Onno C. Goemans, Ken Goldberg and A. Frank Van DerStappen, "Blades: A new class of geometric primitives for feeding 3D parts on vibratory tracks," *Proceedings of the IEEE International Conference on Robotics and Automation*, Orlando, FL (2006).
14. R. Grupen, T. Henderson and I. McCammon, "A survey of general-purpose manipulation," *Int. J. Robot. Res.* **8**(1), 38–62 (1989).
15. L. Joskowicz, E. Sacks and V. Srinivasan. "Kinematic tolerance analysis," *Comput.-Aided Des.* **29**(2), 147–157 (1996).
16. J. Larson and H. Cheng, "Object-oriented CAM design through the Internet," *J. Intell. Manuf.* **11**, 515–534 (2000).
17. J.-C. Latombe, R. Wilson and F. Cazals. "Assembly sequencing with toleranced parts," *Comput.-Aided Des.* **29**(2), 159–174 (1997).
18. K. Lynch, "Toppling manipulation," *Proceedings of the IEEE International Conference on Robotics and Automation*, Detroit, MI (1999), pp. 2551–2557.
19. M. Mason and J. Salisbury. *Robotic Hands and the Mechanics of Manipulation* (MIT Press, Cambridge, MA, (1985).
20. M. Mason, "Two graphical methods for planar contact problems," *Proceedings of the IEEE/RSJ International Conference on Intelligent Robots Systems*, Osaka, Japan (1991), pp. 443–448.
21. B. Mishra, J. Schwartz and M. Sharir, "On the existence and synthesis of multifinger positive grips," *Algorithmica* **2**(4), 541–558 (1987).
22. R. Murray, Z. Li and S. Sastry. *A Mathematical Introduction to Robotic Manipulation* (CRC, Boca Raton, FL, (1994).
23. A. Okamura, N. Smaby and M. Cutkosky, "An overview of dexterous manipulation," *Proceedings of the IEEE International Conference on Robotics and Automation*, San Francisco, CA (2000), pp. 255–262.
24. S. Piccinocchi, M. Ceccarelli, F. Piloni and A. Bicchi, "Interactive benchmark for planning algorithms on the Web," *Proceedings of the IEEE International Conference on Roboticss and Automation*, Albuquerque, NM (1997), pp. 399–404.
25. F. Preparata and S. Hong. "Convex hulls of finite sets of points in two and three dimensions," *Commun. ACM* **20**(2), 87–93 (1977).
26. A. Requicha, "Mathematical definition of tolerance specifications," *Manuf. Rev.* **6**(4), 269–274 (1993).
27. U. Roy, C. Liu and T. Woo, "Review of dimensioning and tolerancing: Representation and processing," *Comput.-Aided Des.* **23**(7), 466–483 (1991).
28. K. Shimoga, "Robot grasp synthesis algorithms: A survey," *Int. J. Robot. Res.* **15**(3), 230–266 (1996).
29. C. Smith and P. Wright, "CyberCut: A World Wide Web based design to fabrication tool," *J. Manuf. Syst.* **15**, 432–442 (1996).
30. G. Smith, E. Lee, K. Goldberg, K. Bohringer and J. Craig. "Computing parallel-jaw grips," *Proceedings of the IEEE International Conference on Robotics and Automation*, Detroit, MI (1999), pp. 1897–1903.

https://doi.org/10.1017/S0263574706003134 Published online by Cambridge University Press

31. A. F. Van Der Stappen, C. Wentink and M. Overmars, "Computing immobilizing grasps of polygonal parts," *Int. J. Robot. Res.* **19**(5), 467–479 (2000).
32. K. Van Katwyk and H. Cheng, "Xlinkage: A Web-based analysis and simulation tool for planar mechanical systems (*CD)*," *Proceedings of the ASME Design Engineering Technical Conference*, Sacramento, CA (1997).
33. H. Voelcker, "A current perspective on tolerancing and metrology," *Manuf. Rev.* **6**(4), 258–268 (1993).
34. R. Wagner, G. Castanotto and K. Goldberg, "FixtureNet: Interactive computer-aided design via the World Wide Web," *Int. J. Hum.-Comput. Stud.* **46**, 773–788 (1997).
35. C. Yap and E. Chang, "Issues in the metrology of geometric tolerancing," In: *Algorithms for Robotic Motion and Manipulation* (J.-P. Laumond and M. Overmas, eds.) (A. K. Peters, Natick, MA, (1997), pp. 393–400.
36. M. T. Zhang and K. Goldberg, "Design of robot gripper jaws based on trapezoidal modules," *Proceedings of the IEEE International Conference on Robotics and Automation*, Seoul, Korea (2001), pp. 1065–1070.
37. M. T. Zhang, L. Cheung and K. Goldberg. "Shape tolerance for robot gripper jaws," *Proceedings of the IEEE/RSJ International Conference on Intelligent Robots Systems*, Wailea, HI (2001), pp. 1782–1787.
38. M. T. Zhang, K. Goldberg, G. Smith, R. P. Berretty and M. Overmars, "Pin design for part feeding," *Robotica* **19**(6), 695–702 (2001).
39. M. T. Zhang, "Optimal design of self-aligning robot gripper jaws," *Ph.D. Dissertation* (Department of Industrial Engineering and Operations Research, University of California, Berkeley, (2001).
40. M. T. Zhang and K. Goldberg, "Gripper contacts for part alignment," *IEEE Trans. Robot. Autom.* **18**(6), 902–910 (2002).
41. M. T. Zhang and K. Goldberg, "Computer-aided gripper jaw design on the Internet," *ASME Trans. J. Comput. Inf. Sci. Eng.*, **4**(1), 43–48 (2004).

https://doi.org/10.1017/S0263574706003134 Published online by Cambridge University Press